Eur. Phys. J. Plus (2025) 140:382
https://doi.org/10.1140/epjp/s13360-025-06281-5

THE EUROPEAN PHYSICAL JOURNAL PLUS

Regular Article

Spatio-temporal monitoring of the microsurface modification in artworks under environmental forcing

Sara Mazzocato[a], **Claudia Daffara**[b]

Department of Computer Science, University of Verona, Strada le Grazie 15, 37134 Verona, Italy

Received: 2 November 2024 / Accepted: 29 March 2025

Abstract Despite the valuable role of surface metrology in engineering, its potential in heritage science remains to be fully recognized. The reasons for this are evident: A hand-made artwork is a complex object with a hand-processed surface and non-homogeneous micro-geometry, subjected to different external stimuli. This study analyses the surface topography of artworks under environmental forcing and proposes a method for the spatio-temporal monitoring of its modification at the micrometer scale, using surface metrology parameters and multiscale techniques. It extends beyond the use of single roughness parameters, with a particular focus on the computation of the power spectral density function of the surface height dataset for estimating the contribution of the different spatial wavelengths to the acquired surface texture signal. As a proof of concept for the practical application of the spectral-based technique, we present two exemplary case studies that evaluate the effect of climate-induced variations on the surface of the artwork. The underlying hypothesis is that the dynamic interplay between scales in climate creates a dynamic interplay at the local scale, with cumulative effects on objects. The first case study focuses on the modifications induced by long-term artificial microclimate variations on bronze mock-ups. The second case study investigates the microclimate shock induced on an ancient parchment from the early eleventh century. This parchment was moved from the vault to the (unclimatized) consultation room in the Capitolare Library in Verona, which is the oldest still active library in the world.

1 Introduction

Surface metrology is a well-established tool in the engineering sector, providing guidelines for the quantitative analysis of surface topography (i.e., micrometer scale surface features). However, it has yet to be fully recognized as a resource in heritage science. Cultural heritage artifacts act as invaluable windows into the past, offering insights into the historical, artistic and scientific achievements of bygone eras. They are often hand-made objects and their peculiarities create a challenge: Unique heterogeneous surfaces require a multiscale approach, and the meaning of surface roughness descriptors in conservation science needs to be clarified [1, 2].

Our group has significantly developed surface profilometry specifically for artwork applications. We have optimized a measurement workflow using a custom laser scanning profilometer based on conoscopic holography, enabling in situ whole-field measurement. This device measures the surface morphology in macro-regions, i.e., order of tens of centimeters, with micrometer accuracy, performs well on both diffusive and highly reflective materials and offers a versatile range of operations. Previously published results have shown the potential of surface metrology in monitoring painting treatments [3] and tackling challenging tasks such as silver treatments when using ISO standard descriptors [4]. Recently, we implemented a methodology for the spatial referencing of the microsurface dataset [5], allowing the scanning of heterogeneous artworks in full-field and conducting reliable surface analysis. In this research, we proposed to use surface metrology, and particularly multiscale techniques, for the spatio-temporal monitoring of the artwork microsurface forced by the external environment.

In this context, developing a suitable data pipeline for investigating complex objects with hand-processed surfaces and non-homogeneous micro-geometry remains critical, mainly where uncontrolled factors influence the surface response. A crucial and demanding aspect of studying cultural heritage assets concerns characterizing surface variations over time as a result of the interaction with external factors, which we call forcing, that cause changes. Artworks are susceptible to deterioration caused by the environment, from a single event like an earthquake [6], to long-term effects like climate variations, with microclimate playing a particularly pivotal role in their preservation or decay [7]. Microclimate refers to the localized atmospheric conditions that can significantly vary within the confines of museums or storage facilities which are not climate-controlled. Often, these local conditions are the result of macroscale variations in climate. Dynamic interactions between global or regional variations in climate will affect local

---

[a] e-mail: sara.mazzocato@univr.it

[b] e-mail: claudia.daffara@univr.it (corresponding author)

microclimates, which may potentially induce cumulative effects on objects. Understanding the impacts on the artwork surface is essential for developing effective conservation strategies and ensuring their longevity, especially in the context of climate change. The attention to this topic has been increasing as demonstrated by European projects, such as Scan4Reco (Multimodal Scanning of Cultural Heritage Assets for their multilayered digitization and preventive conservation via spatio-temporal 4D Reconstruction and 3D Printing) [8], STRENCH (Strengthening resilience of cultural heritage at risk in a changing environment through proactive transnational cooperation) [9], and Hyperion project (Development of a Decision Support System for Improved Resilience & Sustainable Reconstruction of historic areas to cope with Climate Change & Extreme Events based on Novel Sensors and Modeling Tools) [10].

Driven by this motivation, this work aims to move beyond the concept that a surface is a passive object; instead, it can be interpreted as an archive of information that has changed due to spatio-temporal processes, such as environmental factors. It has been shown that the multiscale approach [4] allows a more accurate surface roughness analysis to capture inhomogeneities and understand the scale-limited features that are most informative of the surface response. Here, we discuss the practical application of spectral-based techniques, specifically the computation of the Power Spectral Density (PSD) [11] on surface height datasets forced by microclimate variations. This approach estimates the contribution of different spatial wavelengths to the roughness signal in the acquired artwork's surface texture. Although the multiscale approach has been shown to be effective in monitoring restoration processes [4], its application to climate-induced variations has not been explored.

The proof of concept is given in two distinct heritage materials exposed to climatic variations: bronze and parchment. The paper is structured around three key aspects:

1. Surface monitoring of artificially aged bronze mock-ups;
2. In-line and in situ monitoring of ancient parchment subject to naturally induced microclimate variations;
3. The entanglement of climate processes at multiple scales, from global to micro-environmental.

The choice of materials is meaningful: bronze allows the test of the effects of long-term climate variations, while parchment allows the test of the effects of short-term climate variations.

Bronze artifacts, prevalent in ancient civilizations, are especially vulnerable to corrosion when exposed to fluctuating humidity levels, temperature variations, and pollutants; extensive literature exists, e.g., [12–15]. Outdoor cultural heritage bronze objects are usually protected to slow the corrosion rate [16, 17], and accelerated corrosion conditions are used to test how alloy composition and protective coating properties affect the behavior of bronze [18].

With this in mind, it is clear that monitoring the response of the coated and uncoated surfaces to microclimatic forcing is critical. In literature, the bronze corrosion patinas are inspected through spectroscopic techniques and Scanning Electron Microscope (SEM), e.g. [19], SEM and Optical Coherence Tomography (OCT), e.g. [20], or new approaches such as 3D digital microscopy [13] or fringe projections [21]. In this work, we propose a full-field quantitative surface morphology analysis of wide areas of bronze mock-ups artificially aged, made during the European Project Scan4Reco.

Among cultural heritage, manuscripts are some of the most fascinating objects, having passed from hand to hand over the centuries to the present day. Culture revolutionized from oral and aural to written and visual through writing and text production. By its very nature, a text needs physical support to rest, and one of the most widespread and used since ancient times is parchment. Parchment is a complex natural material made from the skin of animals (goat, sheep, or calf) that has been processed.

Parchment is mainly collagen with some lipids and inorganic matter. Its distinctive structure makes it strong and stable, but it can deteriorate over time due to environmental stresses [22]. Despite the delicate nature of parchment folia, relative humidity (RH) and temperature (T) recommendations for parchment preservation vary widely for libraries and archives, and guidelines with a solid scientific basis are lacking [23, 24].

Small-scale morphological analysis of parchment manuscripts can be found in the literature. For example, in [25], authors investigated the restoration of parchment using SEM images, mercury porosimeter, and water vapor adsorption/desorption isotherms. In [26], a survey of a reference collection of more than 100 historical parchment samples assesses, among other properties, surface roughness. More recently, in [27], researchers proposed a multi-analytic protocol to determine the chemical and morpho-structural characteristics of two old documents on parchment support using SEM coupled by Energy Dispersive X-ray Spectrometry (SEM-EDX).

The adsorption and desorption of water induce small-scale changes that, in turn, cause deformations at larger scales. In literature, only a few studies have investigated the larger scale surface deformations induced on parchment-based manuscripts by moisture changes. In [28], authors analyzed the moisture-induced deformations using a scanner with a laser triangulation sensor, paving the way for exploiting the relationship between the curling and RH variations to derive categories of risk to parchment from indoor climate variations. In [24], authors exploited digital image correlation (DIC) to explore the mechanical behavior of bound volumes to investigate threshold limits for temperature and relative humidity. While, in [29], researchers performed a 3D DIC to monitor the displacements and strains in parchments exposed to environmental changes.

Here, we analyzed the microsurface response of an ancient parchment from the early 11th century to changes in internal micro-climatic parameters (RH, T) induced by changes in the external climate. We had the possibility to work in situ in the Capitolare Library in Verona, the oldest still active library in the world.

2 Materials and methods

2.1 Multiscale analysis

A surface can be conceived as a two-dimensional continuous function of heights sampled by the instrument and then represented as a discrete function. The choice of the instrument affects the lowest and the upper observable scale. Our research group has concentrated its efforts on developing multiscale analysis techniques suitable for cultural heritage applications. We have identified three principal aspects in multiscale analysis: scale inspection, signal separation, and in-band analysis.

Scale inspection aims to thoroughly study the variation of the surface in sub-regions by evaluating the behavior of parameters in each sub-area and varying its length scale. This approach is particularly relevant in the case of non-homogeneous hand-made objects or to monitor random processes. Surfaces are inherently multiscale and can be understood as composites of shape and texture. Furthermore, texture can be conceived as consisting of waviness and roughness. Signal separation allows the decomposition of the texture signal into waviness and roughness by using different thresholds through a Gaussian filter with different cutoff values. This procedure enables the study of roughness parameters in scale-limited surface components. Both methodologies have been proven effective in [4].

In this paper, as much as both scale inspection and signal separation are used, special focus is placed on the in-band analysis.

The surface roughness PSD represents the spatial frequency-domain distribution of surface irregularities, providing information about the intensity of such irregularities at different spatial wavelengths λ_i. From a statistical point of view, the PSD and the probability density distribution of heights provide the most comprehensive information on surface roughness [30], giving information about the spatial arrangement and the out-of-plane changes, respectively. The PSD is commonly used in surface metrology and engineering fields to perform quality control, study adhesion, friction, and wear [31, 32] or to solve measurement errors [33].

The PSD of a rough surface, commonly referred as $C(\mathbf{q})$, is defined as:

$$C(\mathbf{q}) = \frac{1}{(2\pi)^2} \int_A \langle z(\mathbf{x}) z(\mathbf{0}) \rangle e^{-i\mathbf{q}\cdot\mathbf{x}} \mathrm{d}\mathbf{x}\,, \tag{1}$$

where $z(\mathbf{x})$ is the height at the coordinate $\mathbf{x} = (x, y)$, $\langle \ldots \rangle$ is the ensemble average, and $\mathbf{q}$ is the wavevector, with $q_i = 2\pi/\lambda_i$.

Going beyond the concept of the artwork as a static object, its surface can be considered an ever-changing system due to its interaction with the external environment, with the spatial and time scales of these changes depending on the type of phenomena involved. Monitoring a surface in time and analyzing it through the PSD highlights details about how the different spatial wavelengths change over time, revealing the nature of the scale involved.

It is known that the roughness Sq is the squared root of the area under the PSD [31]. Thus, we define the in-band roughness in a frequency range $[q_1, q_2]$, as follows:

$$Sq^2_{[q_1,q_2]} = \int_{q_1}^{q_2} C(q)\mathrm{d}q\,. \tag{2}$$

This approach allows to inspect the most impacted spatial wavelengths in relation to the forcing processes.

2.2 Environmental forcing experiments and profilometry dataset

To effectively acquire the texture of different surfaces at the micrometer scale and thus sample meaningful information on roughness and waviness, a microprofilometry technique is needed that maintains a good signal-to-noise ratio over diverse materials, has high resolution in both depth (sub-micron) and lateral (micron) directions, as well as the ability to scan in full-field (tens of centimeters). For this purpose, we optimized and used a customized portable microprofilometer relying on single-point interferometric depth sensors based on conoscopic holography and micrometer linear stages with a maximum scan size of 30 cm × 30 cm and a minimum incremental motion of 0.1 µm. The optical probe measures the distance in the direction of the line of sight, orthogonal to the xy scanning grid.

To sample the bronze mock-ups, the optical scanner microprofilometer was equipped with the ConoPoint3-HD coupled with a 50 mm focal lens, enabling repeatability, i.e., the standard deviation of 10000 static measurements, that varies from 1 µm to 1.9 µm over the set of samples, with a mean value of 1.4 µm. In the case of parchment, the ConoPoint3 coupled with a 50 mm focal lens was chosen to provide a wider working range to account for the depth deformations. The measured repeatability in the ancient parchment is 0.9 µm, while in the modern parchment is 1 µm. Each object was sampled with a scan step of 50 µm and a scan velocity of 10 mm/s.

2.2.1 Forcing due to long-term climatic variations: bronze

During the Scan4Reco project, the *Opificio delle Pietre Dure* guided by the ISO standards and the literature, tested the effect of bronze aging due to the variation of external environmental parameters (i.e., sunlight, humidity, rain, and heat). The bronze specimens (8 × 5 cm^2 in size and 4 mm thick) were created with a representative alloy used in the arts, that is 90% copper and 10% tin. Table 1

Table 1 Bronze samples and applied coatings

Sample	1	2	3	4	5
Protective coating	Uncoated	Incral44	Reswax (Ligroin)	Reswax (Isooctane)	Paraloid B44

Fig. 1 Visible image of sample 5 (coated with Paraloid B44) evolution over time. From left to right: time 0 (before aging), time 1 (6 weeks), time 2 (12 weeks)

Fig. 2 Visible image of the ancient parchment with the analyzed ROI highlighted

details the samples and the respective applied protective coatings selected because they are the most common in the conservation community.

An aging chamber equipped with an ultraviolet (UVA) fluorescent lamp, moisture condensation device, and water spray (QUV chamber) was used. The temperature range of the chamber is 50 °C to 75 °C, while the condensation temperature is 40 °C to 60 °C. The applied cycle is as follows: 4 h of dry conditions (T = 60 °C) and UV exposure to simulate sunshine exposure, 4 h of wet conditions (T = 40 °C, RH = 90%), manual spraying every six cycles with solution[1] for imitating an acid rain [34].

The total time of the aging was 12 weeks, and the mock-ups were acquired before the aging (time 0), after six weeks (time 1), and at the end of the process (time 2). In addition, we measured the samples after nearly eight years (time 3), when the samples were stored in a box and experienced natural aging (ambient RH and T). Figure 1 provides the visible images of sample 5, selected for illustrative purposes, over time of artificial aging.

2.2.2 *Forcing due to short-term microclimatic variations: ancient parchment*

In this research, we propose a new approach to monitor the surface of an ancient parchment using the optical microprofilometer. In particular, we worked in situ at the *Capitolare Library*, the oldest still active library in the world.

The case study is a restored parchment dated 1082 A.D., as illustrated in Fig. 2. The document consists primarily of original ancient parchment, with certain areas of modern parchment that have been grafted and glued to the original to fill the gaps.

The parchment is stored in a vault devoid of an active climate control system. However, RH and T are passively controlled due to the architectural features of the building. The RH is relatively stable, with a typical value of approximately 55%. The aim is

---

[1] Solution composition: Cl^- (1.27 mg/L), NO_3^- (4.64 mg/L), NH_4^+(1.06 mg/L), $SO_4^=$ (1.9 mg/L), $HCOO^-$ (0.05 mg/L), CH_3COO^- (0.23 mg/L), Na^+ (0.53 mg/L), Ca^{2+} (0.34 mg/L), pH=4.25.

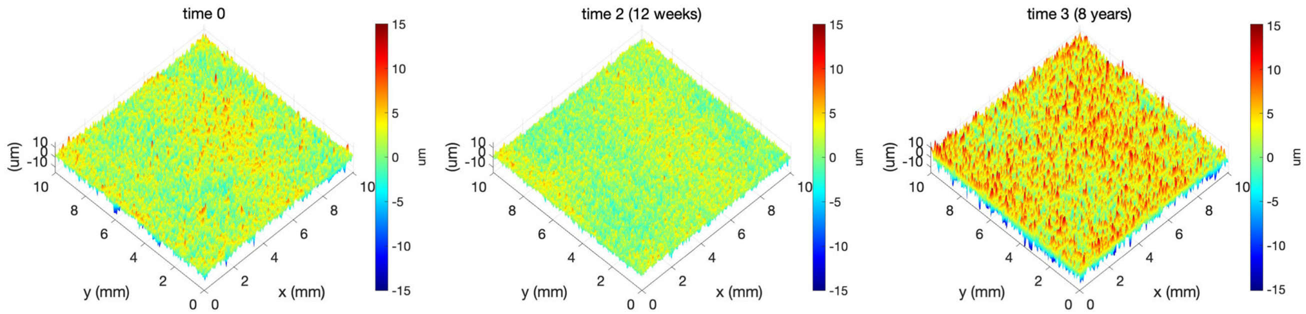

(a) Sample 1: $Sq_{t0} = (3.07 \pm 0.03)\mu m$, $Sq_{t2} = (2.40 \pm 0.03)\mu m$, $Sq_{t3} = (5.04 \pm 0.05)\mu m$

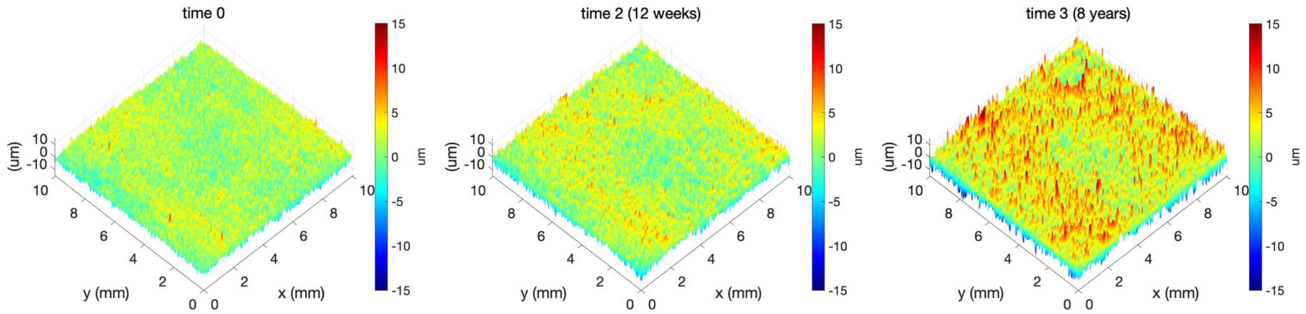

(b) Sample 5: $Sq_{t0} = (2.17 \pm 0.02)\mu m$, $Sq_{t2} = (2.82 \pm 0.03)\mu m$, $Sq_{t3} = (4.53 \pm 0.05)\mu m$

Fig. 3 Representative ROI of 1 cm^2 visualized in the same scale (3-sigma of time 3 from the mean) for comparison

Table 2 Roughness values over time calculated in the 1 cm^2 ROI

Sample Coating	1 Uncoated	2 Incral44	3 Reswax (Ligroin)	4 Reswax (Isooctane)	5 Paraloid B44
Sq_{t0} (μm)	3.07 ±0.03	2.22 ±0.02	2.14 ±0.02	1.96 ±0.02	2.17 ±0.02
Sq_{t2} (μm)	2.40 ±0.03	2.79 ±0.03	2.73 ±0.03	2.69 ±0.03	2.82 ±0.03
Sq_{t3} (μm)	5.04 ±0.05	4.38 ±0.04	4.39 ±0.05	4.47 ±0.05	4.53 ±0.05

the study of the multiscale surface response in actual consultation conditions, i.e., when the document is brought from the vault to the consultation room. This room is more susceptible to environmental variations during the year due to its position within the building and due to the presence of a constant flow of people. This change in rooms leads to environmental changes and, thus, to forcing factors on the surface. For such a hygroscopic object, the predominant forcing factor is the variation in relative humidity. In principle, due to the in-plane and through-thickness moisture content gradient, in-plane and out-of-plane deformations can be expected. In our case, deformations in *xy* plane are negligible compared with out-of-plane deformations, as found by comparing the Total maps, i.e., the maps of the intensity of signal collected by the sensor [5].

The experiment was conducted over three days: on the first day, the scroll was moved from the vault to the consultation room, and the ROI was measured. The same ROI was then acquired after two days in which the parchment remained in the same room and underwent climate forcing.

3 Results

3.1 Forcing due to long-term climatic variations: bronze

Figure 3 shows the texture of a representative ROI of 1 cm^2 of samples 1 (uncoated) and 5 (coated with Paraloid B44) at time 0, time 2, i.e., at the end of the artificial aging process, and time 3, i.e., after eight years of natural aging. The ROIs are located in the central part of the samples to select a region with an approximately homogeneous coating distribution and avoid accidental holes or scratches.

Table 2 reports the roughness values Sq in the aging steps for all the samples.

Table 3 Scale inspection of a 30 mm × 30 mm ROI for each sample

Sample	time 0	time 2 (12 weeks)	time 3 (8 years)	PSD
1 - uncoated	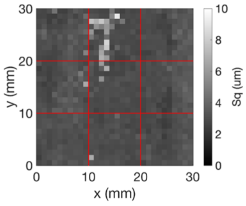	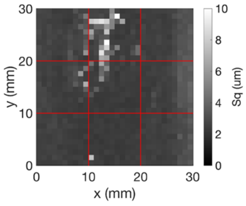	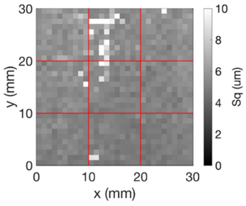	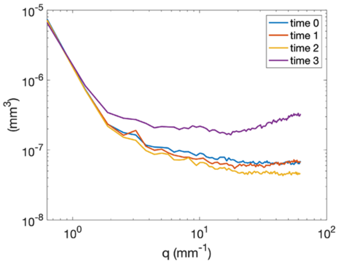
2 - Incral44	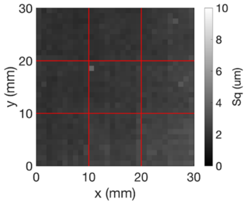	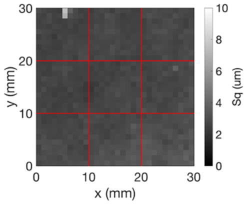	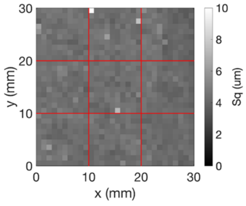	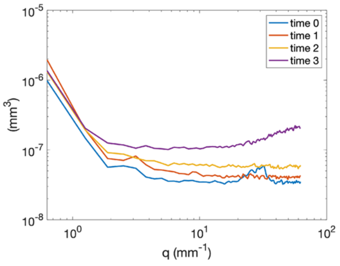
3 - Reswax (Ligroin)	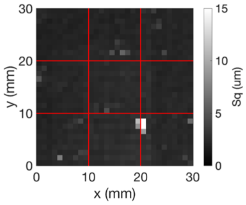	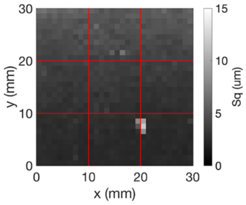	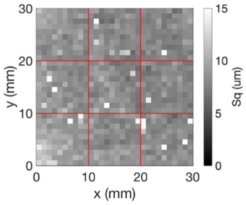	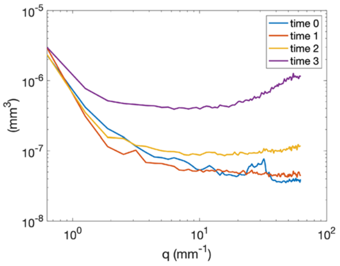
4 - Reswax (Isoctane)	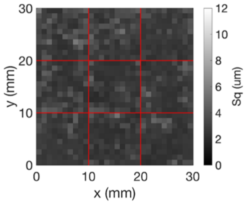	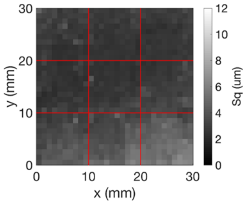	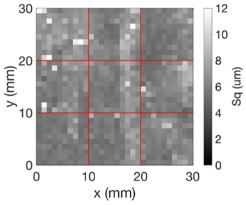	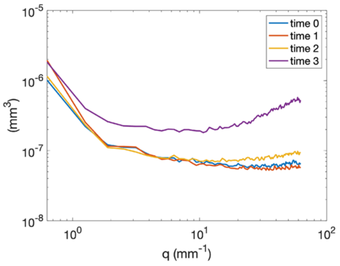
5 - Paraloid B44	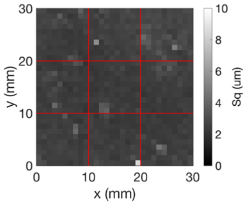	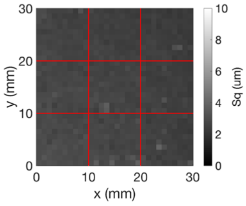	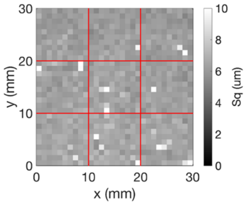	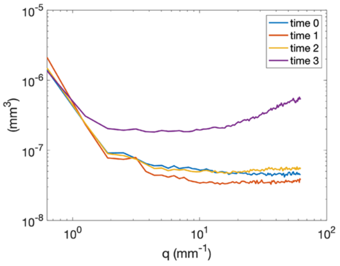

The last column provides the 1 cm^2 ensemble averaged PSD over time, plotted in the same range for comparison

Table 3 shows the variation of the roughness averaged over a sub-patch of 1 mm^2 of a central ROI of 30 mm × 30 mm for each sample.

The *xy* scale inspection, proposed by the authors in [4], provides an insight into the local distribution of the parameters over the whole analyzed surface. In this way, on the one hand, it is possible to visually identify the inhomogeneities of the sampled surface. On the other hand, the comparison with another surface, or the same surface over time, based on its roughness signature is more straightforward. However, what cannot be inferred from the inspection of the local distribution of the roughness values is the

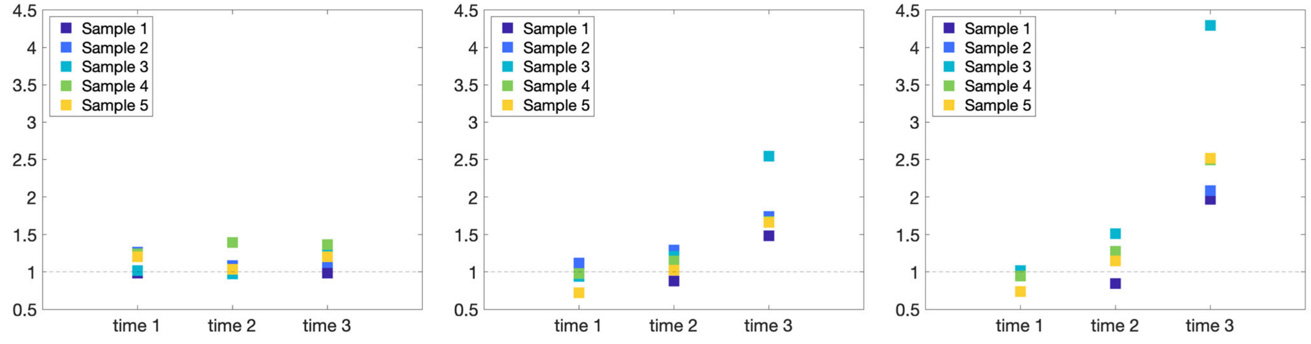

(a) λ range: 10 mm to 3.3 mm (b) λ range: 3.3 mm to 0.36 mm (c) λ range: 0.36 mm to 0.1 mm

Fig. 4 In-band roughness ratio between the value at time 0 and the values at time 1,2,3 (6 weeks, 12 weeks and 8 years, respectively) for each sample in the three selected λ-range

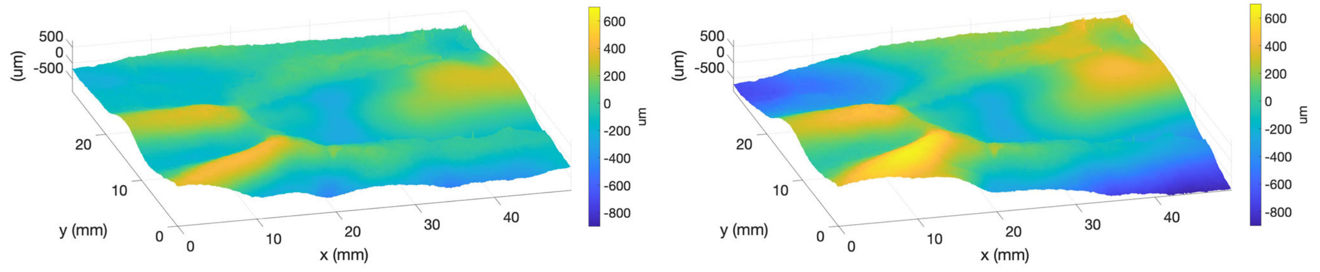

(a) time 0 (day 1) (b) time 1 (day 3)

Fig. 5 3D representation of the heights map of the ROI at the beginning (**a**) and after two days (**b**)

multiscale nature of the surface, i.e., the scale-limited contribution in the different spatial bands. The PSD clarifies this. The table gives the patch-based ensemble PSD for each sample, i.e., the PSD averaged over patches of 1 cm^2 highlighted with red lines. This ensemble approach allows for mitigating the contribution of inhomogeneities to the PSD, which thereby contains information on the main features from the ROI size up to twice the sampling step. It is interesting to note the different impacts of artificial aging (time 0,1,2) and natural aging (time 3): for each sample, the surface signal at time 3 is higher than the older respective signals. Moreover, the PSDs emphasize the effect of the different coatings. For example, samples 2 and 3 show a peak at $q \simeq 30$ mm^{-1} ($\lambda \simeq 0.2$ mm). This effect is then smoothed out during the time, as can be seen by the peak dampening. This behavior suggests inhomogeneity due to the layering of the coating that disappears once the aging process leads the layer to adapt more effectively to the surface morphology.

Figure 4 shows the calculated in-band roughness ratio. The proposed λ-range are 10 mm to 3.3 mm, 3.33 mm to 0.36 mm, and 0.36 mm to 0.10 mm (0.63 mm to 1.89 mm^{-1}, 1.89 mm to 17.59 mm^{-1}, and 17.59 mm to 62.20 mm^{-1}, respectively), selected on the basis of the PSD plots. For each λ-range, the plot shows the ratio of the in-band roughness at time 1,2 and 3 ($Sq_{[q_1,q_2],t}$) relative to the respective in-band roughness at time 0 ($Sq_{[q_1,q_2],t_0}$). As can be seen, the smaller scales are the most impacted, especially at time 3.

3.2 Forcing due to short-term microclimatic variations: ancient parchment

The ROI highlighted in Fig. 2 was scanned in the context of natural microclimatic variation induced by external climatic changes. The choice of the area is meaningful: it is a restored part of the document in which there is the simultaneous presence of the ancient and modern parchment. The measurements were performed over three days, the first one after the rapid parchment relaxation phase and the other one after two days. Figure 5 shows the 3D representation of the scanned surface at the beginning (time 0) and after two days (time 1).

Several sensors were placed in the library to monitor the microclimate conditions. Figure 6 shows the trends of the RH and the temperature: The blue line represents the data of the sensor placed in the vault and subsequently moved with the parchment to the consultation room. The yellow line corresponds to the data of sensor placed outside the building. As expected, there is a delay in the increase in humidity inside the consultation room, with an estimated 6.5-hour time lag in the RH peak.

Over time, the surface changed in response to the alteration of the indoor microclimate conditions. The main challenge is to perform a meaningful analysis of these changes. Overall, the Sq value of the texture signal, i.e., the sum of the waviness and

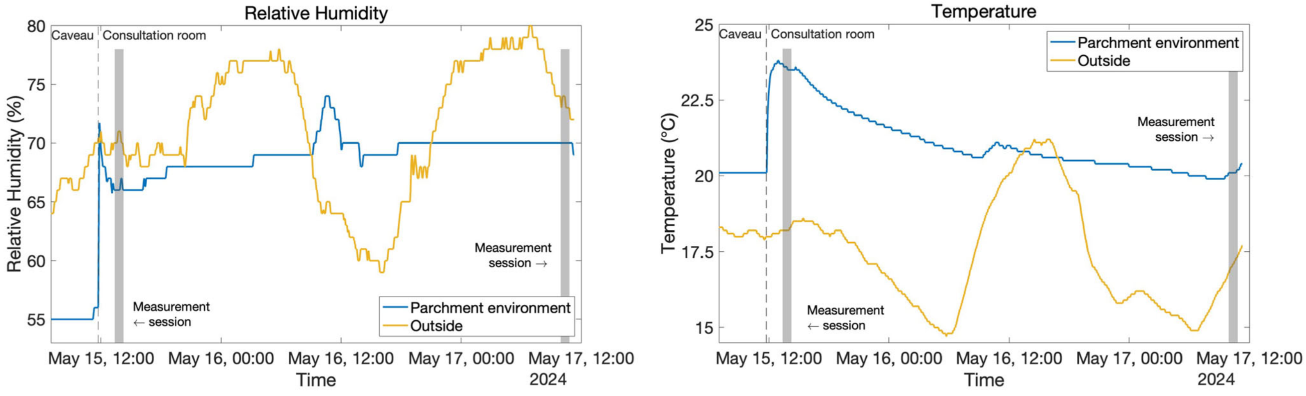

(a) (b)

Fig. 6 Plots of the RH and temperature. The blue lines represent the measurements of the sensor that is moved from the vault to the consultation room, while the yellow lines represent the measurements of the sensor placed outside the building. The nominal errors of the sensors are ± 1.8% in RH, and ± 0.2 °C in temperature

Table 4 Comparison of surface roughness Sq of the entire scanned surface with the Sq calculated for the ancient and modern parts

	Time 0 (day 1)	Time 1 (day 3)
Entire ROI Sq (µm)	167.7 ± 0.5	300 ± 0.8
Ancient part Sq (µm)	166.7 ± 0.5	329.2 ± 0.9
Modern part Sq (µm)	161.2 ± 0.4	205.2 ± 0.6

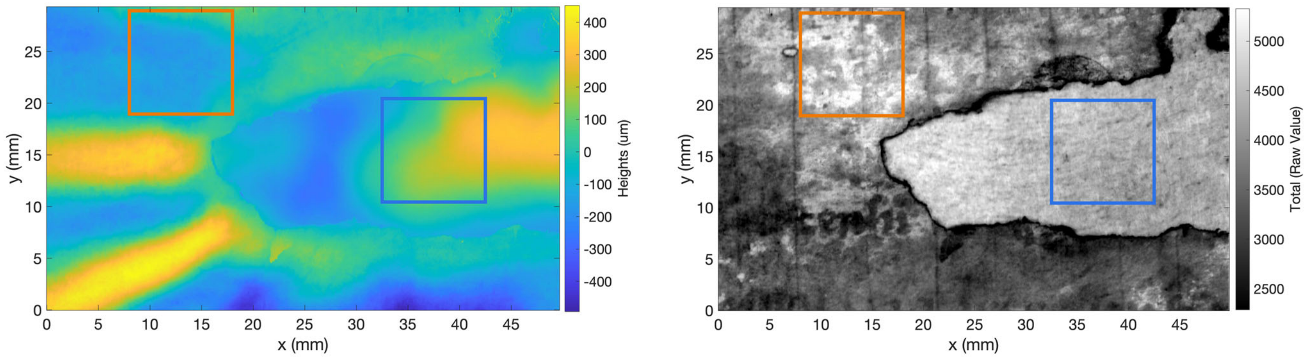

(a) Height map - time 0 (b) Total map - time 0

Fig. 7 Height map (**a**) and Total map (**b**) of the ROI at time 0; the sub-ROIs of the old and modern parchment are highlighted

roughness, changes as reported in Table 4. However, calculating the single roughness parameter over a large area, including depth deformations that may occur as in the case of hygroscopic materials, can lead to misleading results. For this reason, we performed a deeper in-band analysis of two representative sub-ROIs.

Figure 7 shows the two selected sub-ROIs for the power spectral analysis. Figure 7a represents the height map of the scanned surface, while Fig. 7b is the map of the Total values, that is, the intensity of signal collected by the sensor. As demonstrated by the authors in [5, 35], the Total map allows the surface to be interpreted and, hence, to perform a meaningful segmentation.

To monitor only the finer scale, the shape of each single ROI was removed through a least-squares fit of the second-order polynomial. Figure 8 shows the averaged 1D-PSD along scan direction for the ancient and modern parchment. As can be seen, there is a generally different curvature of the PSD for the ancient and modern parchment, and the spatial wavelengths most affected are the higher ones. The dashed lines are in correspondence with λ values of 0.10 mm, 0.31 mm, 0.63 mm, 2.5 mm, and 10 mm, respectively. These values are deemed the most representative of the spatial wavelength bands in which the signals vary. Figure 9 shows the ratio of the in-band roughness after and before the forcing ($\mathrm{Sq}_{[q_1,q_2],day3}/\mathrm{Sq}_{[q_1,q_2],day1}$). It emerges that the range between 0.10 and 0.31 mm is the most affected range, with a decrease in the in-band roughness. It is worth noting that the old parchment is more affected than the modern parchment. The range between 0.63 and 2.5 mm remains almost unaltered, while the range between 2.5 and 10 mm shows a slight increase in the roughness over time.

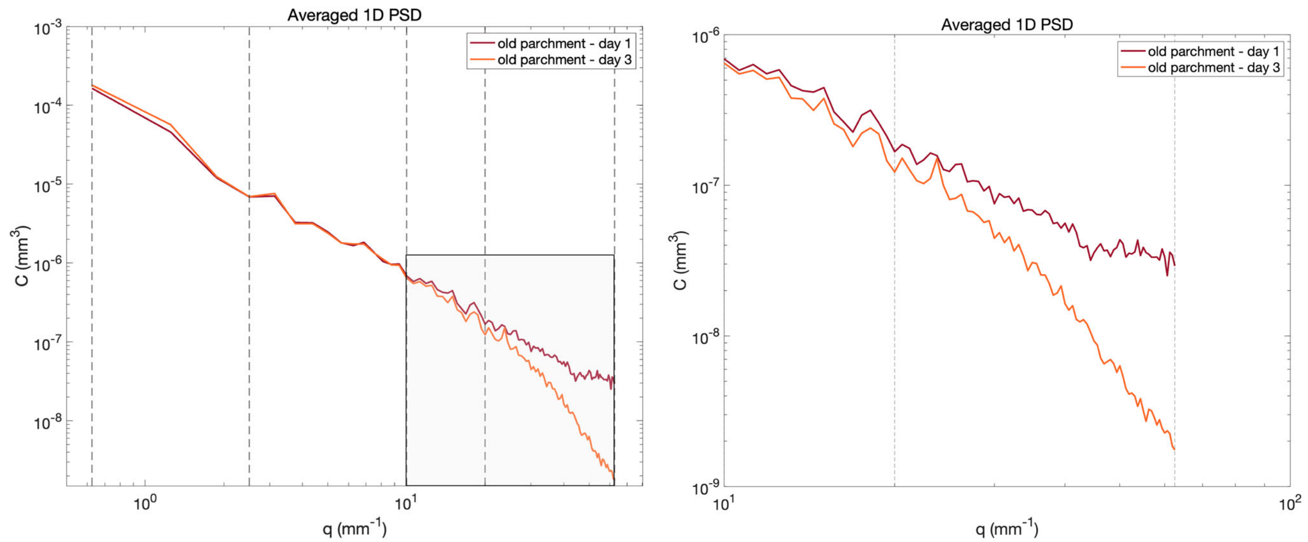

(a) ancient parchment

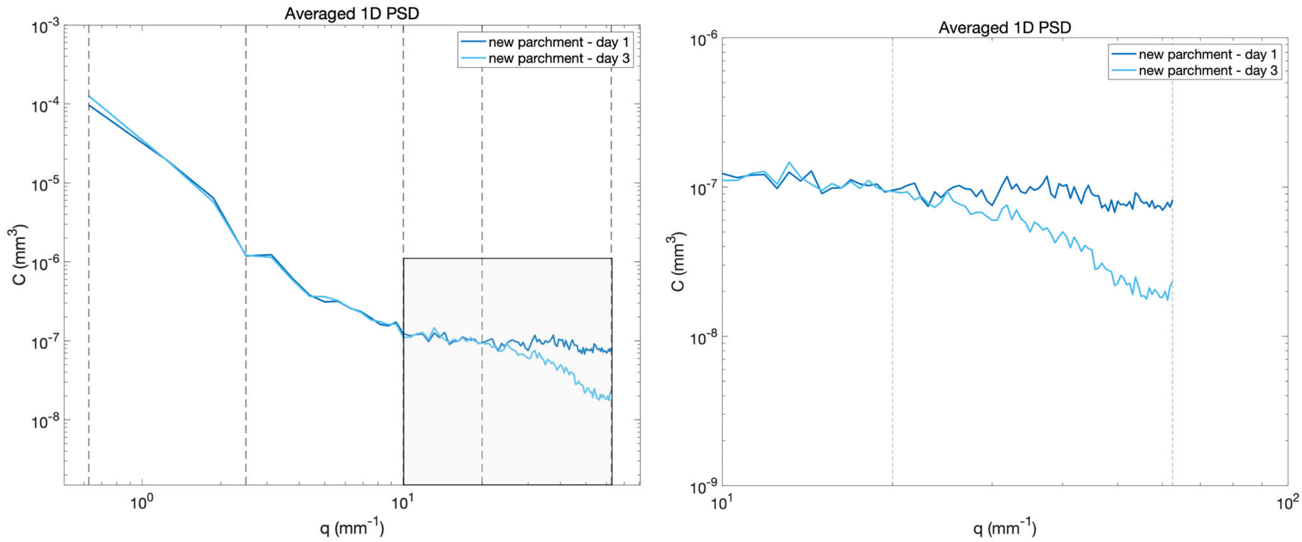

(b) modern parchment

Fig. 8 PSD function of the ancient and the modern parchment over time. The function is calculated as 1D averaged PSD along the scan direction. The dashed lines define the limits of the most significant identified bands. They are in correspondence with λ values of 0.10 mm, 0.31 mm, 0.63 mm, 2.5 mm, and 10 mm, respectively

The above behavior can be visually inspected in Fig. 10. The texture (waviness and roughness) of the modern and ancient parchment patches are separated by a Gaussian filter with a cutoff of 0.3 mm selected based on the PSD, which allows for the selection of the most significant scale-limited surface components. If roughness Sq was calculated on the individual patch, the results would indicate the same roughness of 26.3 μm on both the first and third days for the old parchment and a slight change in the modern one from 22.3 to 24.0 μm. The PSD and subsequent signal separation clearly show that the waviness remains very similar, but the finer scales are impacted.

3.3 A glimpse into multiscale climate variations

The days on which the parchment was measured were notable for the occurrence of heavy rainfall in northern Italy. In the context of climate change, extreme precipitations are likely to increase [36], with varying intensity depending on the future scenario. As for Italy, although there is some uncertainty in identifying the most affected areas, a clear trend toward exacerbating weather conditions

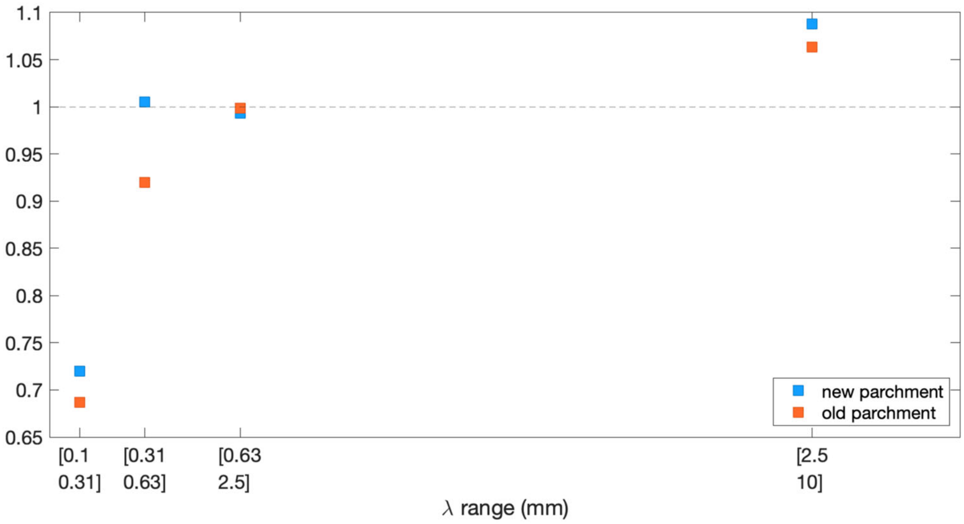

Fig. 9 In-band roughness analysis of the old and new sub-ROIs of parchment. On the y axis the ratio between the in-band roughness of day 3 and day 1 ($\mathrm{Sq}_{[q_1,q_2],day3}/\mathrm{Sq}_{[q_1,q_2],day1}$)

in northern regions is emerging [37]. As macroscale climate is reflected on smaller and smaller scales, the question arises as to whether and how these induced changes involve forcing on the objects that are subjected to them. Figure 11 offers a glimpse of the precipitation pattern over the North of Italy thanks to the dataset ERA5-Land Daily Aggregated provided by Copernicus Climate Data Store [38]. In the maps, the closest stations to Verona, managed by ARPAV (Veneto Regional Agency for Environmental Prevention and Protection) [39], are highlighted.

Figure 12 gives an overview of the evolution of the amount of precipitation, humidity, and temperature recorded by the stations, and the corresponding relative humidity and temperature recorded by the sensor placed outside the window of the room in the Capitolare Library.

It is worth noting that the sensor was placed between the window and the wood shutters, which explains the difference in the intensity and the slight delay of 1 h to 2 h of the variations of the data. The nearest weather station to Verona (Santa Caterina, $\simeq$ 4.5 km from Capitolare library) reports a total precipitation sum of 28.8 mm on the 15th of May, 27.0 mm on the 16th, and 0.2 on the 17th. The minimum relative humidity varies, respectively, from 69%, 68%, and 83% (up to the final measurement session), with a maximum value of 100% in all three days. The other stations are in a range of 7 km to 15 km from the Capitolare, defining the area of macroscale urban climate variations.

Macroscale climate variation, such as global temperature shifts and changing weather patterns, profoundly impacts microscale climate variation, particularly within localized environments like buildings. The multiscale and complex nature of climate means that changes at the global or regional level cascade down to influence local microclimates, creating a dynamic interplay between scales. In the experiment shown, we demonstrated how an extreme weather event impacts the inside of a historical building, influencing how heat and moisture are exchanged between the interior and exterior and ultimately affecting the objects stored inside. This underscores the need to consider the interconnection of climate processes on different scales, from global to micro-environmental.

4 Discussion and conclusion

In this work, we aimed to demonstrate the potentialities of surface metrology in monitoring the spatio-temporal response of the artwork surface forced by climatic variations, focusing on overcoming the usual practice of inspecting the surface structure through single roughness parameters. The artwork's surface can be interpreted as a complex structure resulting from centuries of history, which is expressed in a complex and multifaceted surface topography. From this inherent nature comes the need to use multiscale surface analysis methods. We have selected two exemplary case studies involving two materials as proof of concept. The first case regards artificial long-term climatic variations induced on bronze mock-ups, while the second one concerns the natural short-term climatic variations induced on ancient parchment. In this context, the climate, and in particular the microclimate, is interpreted as a surface modifying forcing, which in the second case allows a glimpse into the inherent multiscale nature of the climate. All the surfaces were measured over time using the optical microprofilometer, which enables significant ROIs to be scanned while maintaining high depth accuracy. In both cases, the multiscale analysis has been proven effective in highlighting the modifications induced by the microclimate alterations. As demonstrated, such surface changes occur primarily at the smaller scales.

In the case of bronze, we monitored the surfaces of five samples, coated and uncoated, artificially aged over a period of 12 weeks plus an additional measure after nearly 8 years. The microprofilometer was able to capture microsurface modifications over time, and the multiscale approach allowed a more reliable analysis of surface roughness, both in terms of texture inhomogeneities as well as for understanding the significant scales involved. This controlled step experiment demonstrated how microclimate can

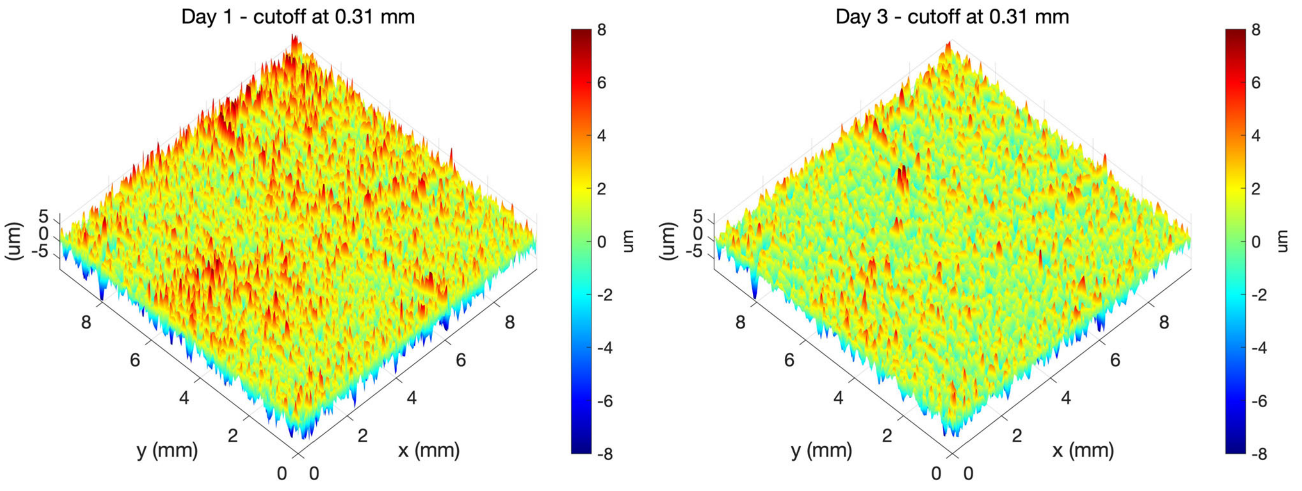

(a) Ancient parchment

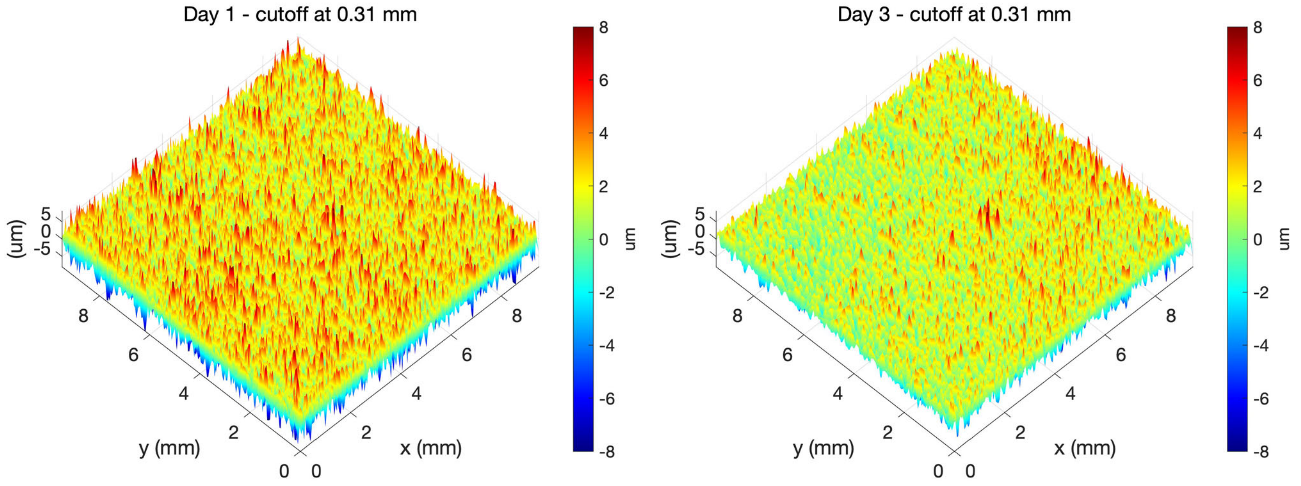

(b) Modern parchment

Fig. 10 Signals separation performed with a cutoff of 300 μm to emphasize the evolution of the roughness over time

induce random cumulative effects on the surface. Consequently, analysis based on average methods rather than local parameters is meaningful.

In the parchment case study, the microclimate was monitored in order to ascertain how it impacted the ancient document during the consultation process. Indeed, the scroll was moved from its original location, which was the vault, to a completely different climatic environment, i.e., the consultation room. We monitored a significant ROI of a manuscript where old and new parchments were present. The twofold goals were: first, to determine that the power spectrum was a suitable tool for detecting changes due to varying microclimatic conditions, and second, to test how modern and ancient parchment responded differently to the same forcing. The PSD analysis highlights how modern and ancient parchment, different even in their signal, respond differently in the various spatial frequencies. It has been shown how calculating surface roughness as a single parameter is misleading. The roughness of ancient parchment has a very similar value before and after climatic stress, thus bringing to the erroneous assumption that there were no significant changes in the finer scale signal. However, the use of the PSD clearly shows that the roughness changes over time outlining the different contributions in the different spatial frequency bands.

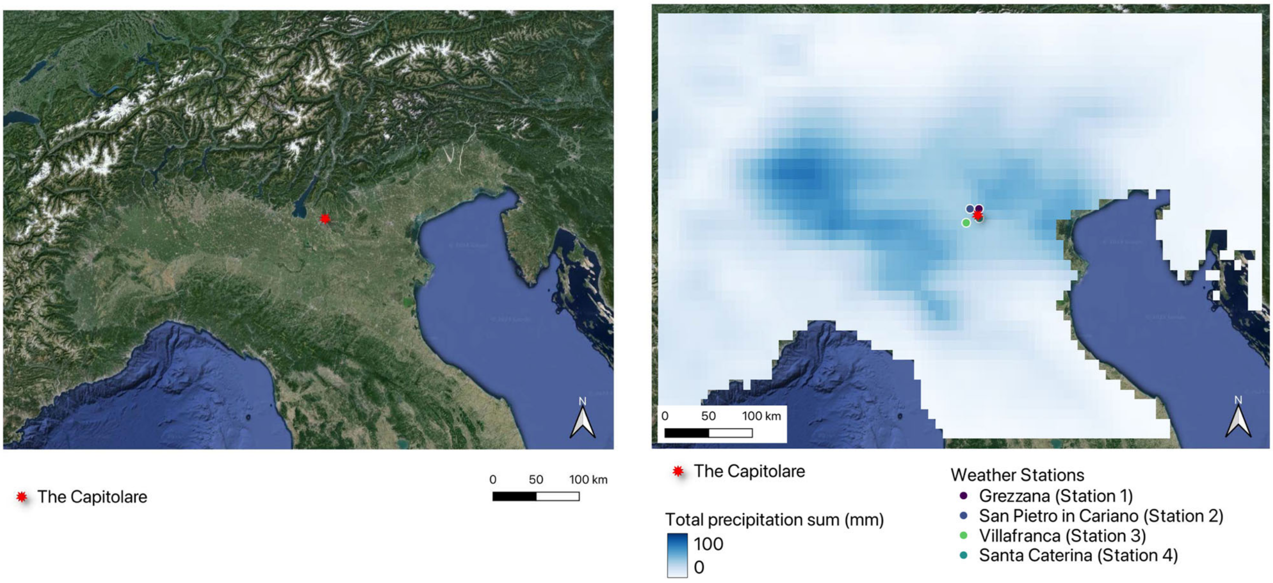

(a) (b) 15th May 2024

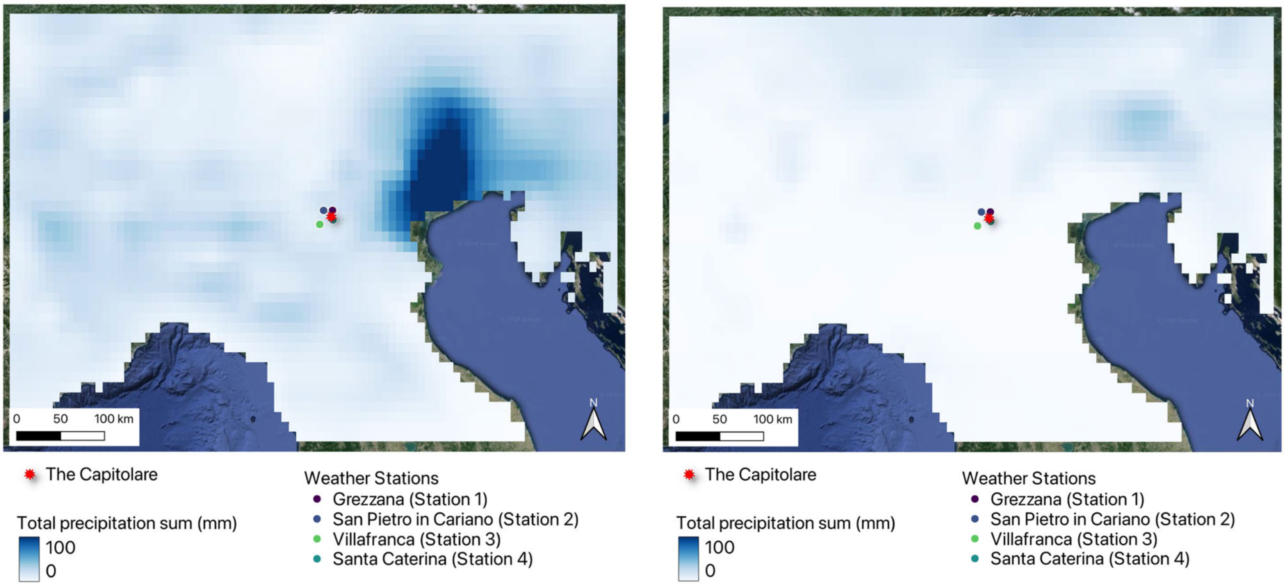

(c) 16th May 2024 (d) 17th May 2024

Fig. 11 Daily aggregate ERA5 Land hourly dataset of the accumulated liquid and frozen water over the north of Italy from May 15th to 17th (2024) [38]

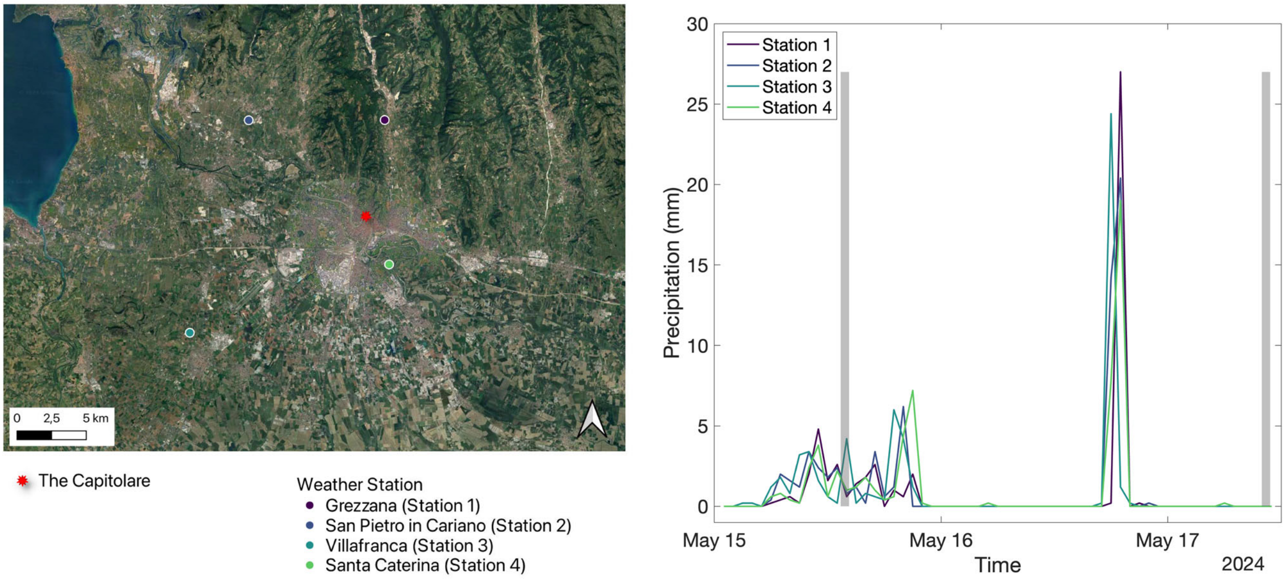

(a) Weather stations map (b) Precipitation

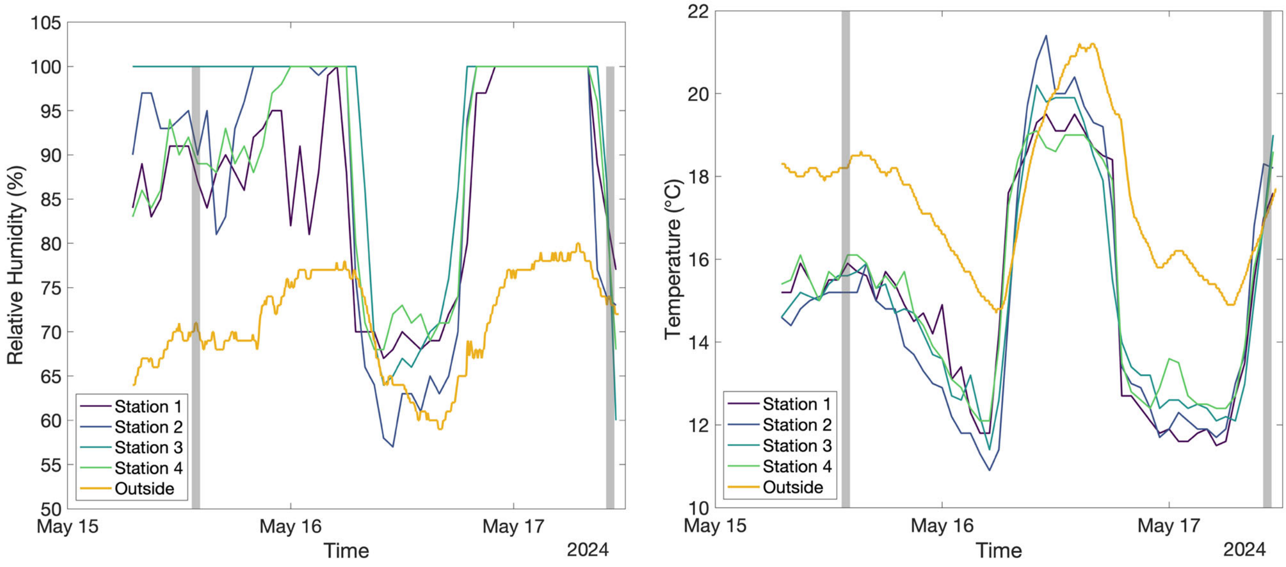

(c) Relative Humidity (d) Temperature

Fig. 12 **a** Locations of the weather stations and the Capitolare. **b** Precipitation. **c** The minimum RH recorded by the stations (at 2 m height) and the RH outside the window of consultation rooms (in yellow). **d** The mean temperature recorded by the stations (at 2 m height) and the temperature outside the window of consultation rooms (yellow). The nominal errors of the sensor placed outside are ± 1.8% in RH, and ± 0.2 °C in temperature. The gray bars represent the measurement sessions

Finally, we exploited open-access climate data, i.e., the macroscale ERA5 data and the mesoscale ARPA weather stations data, to relate the external climate conditions at different scales. The experiment showed that extreme weather events could have a cascading effect on the microscale, particularly on the artwork's microsurface. In future research, we will examine these intriguing findings further, exploring the interpretation of the microsurface as an archive.

Acknowledgements The authors would like to acknowledge Dr. Monica Galeotti (Opificio delle Pietre Dure) for realizing the artificially aged bronze mock-ups and Dr. Giacomo Marchioro (University of Verona) for the measurements with the profilometer, within the Scan4Reco project. The authors would also like to acknowledge the Foundation of the Biblioteca Capitolare of Verona for providing the ancient manuscript. We acknowledge the use of ERA5-Land as stated in the Copernicus C3S/CAMS License agreement: Contains modified Copernicus Climate Change Service information (2024). Neither the European Commission nor ECMWF is responsible for any use that may be made of the Copernicus information or Data it contains.

Funding Open access funding provided by Università degli Studi di Verona within the CRUI-CARE Agreement. This research was funded partly by European Union—NextGenerationEU, PRIN PNRR 2022 Project "Artificial Intelligence and Physics for Art Diagnostics (AIPAD): the killer application of the historical manuscripts and palimpsests", P2022SFEPN—CUP B53D23029240001—Grant Assignment Decree No. 1372 (1/9/2023) by the Italian MUR, and partly by Scan4Reco project, European Union Horizon 2020 Framework Programme for Research and Innovation, under grant agreement No. 66509.

Data Availability Statement Data are available on reasonable request. The manuscript has associated data in a data repository

References

1. X. Jiang, P.J. Scott, D.J. Whitehouse, L. Blunt, Paradigm shifts in surface metrology. Part II. The current shift. Proc. Royal Soc. A: Math. Phys. Eng. Sci. **463**(2085), 2071–2099 (2007). https://doi.org/10.1098/rspa.2007.1873
2. C. Daffara, S. Mazzocato, G. Marchioro, Optical surface metrology for heritage science: proof of concept and critical-constructive discussion. Proc. SPIE **12620**, 126200 (2023). https://doi.org/10.1117/12.2675055
3. C. Daffara, S. Mazzocato, Surface metrology based on scanning conoscopic holography for in situ and in-process monitoring of microtexture in paintings. Sensors **22**(17), 6637 (2022). https://doi.org/10.3390/s22176637
4. C. Daffara, S. Mazzocato, G. Marchioro, Multiscale roughness analysis by microprofilometry based on conoscopic holography: a new tool for treatment monitoring in highly reflective metal artworks. Eur. Phys. J. Plus **137**(4), 430 (2022). https://doi.org/10.1140/epjp/s13360-022-02605-x
5. S. Mazzocato, C. Daffara, A method for spatially registered microprofilometry combining intensity-height datasets from interferometric sensors. Sensors **23**(8), 4144 (2023). https://doi.org/10.3390/s23084144
6. E. Vannini, I. Lunghi, E. Grifoni, P. Farioli, M. Ginanni, A. Santacesaria, R. Fontana, Three-dimensional analysis for the documentation of the restoration of an earthquake-damaged triptych. Heritage **7**(4), 2176–2194 (2024). https://doi.org/10.3390/heritage7040103
7. D. Camuffo, *Microclimate for Cultural Heritage*, 3rd edn. (Elsevier Science, London, England, 2019)
8. Scan4Reco - Multimodal Scanning of Cultural Heritage Assets for their multilayered digitization and preventive conservation via spatiotemporal 4D Reconstruction and 3D Printing. https://scan4reco.iti.gr. [Accessed 23-08-2024]
9. STRENCH - Strengthening resilience of cultural heritage at risk in a changing environment through proactive transnational cooperation. https://programme2014-20.interreg-central.eu/Content.Node/STRENCH.html. [Accessed 23-08-2024]
10. Hyperion Project (Development of a decision support system for improved resilience & sustainable reconstruction of historic areas to cope with climate change & extreme events based on novel sensors and modelling tools). https://www.hyperion-project.eu. [Accessed 23-08-2024]
11. A. DuparrÃ©, J. Ferre-Borrull, S. Gliech, G. Notni, J. Steinert, J.M. Bennett, Surface characterization techniques for determining the root-mean-square roughness and power spectral densities of optical components. Appl. Opt. **41**(1), 154 (2002). https://doi.org/10.1364/ao.41.000154
12. P. Letardi, B. Salvadori, M. Galeotti, A. Cagnini, S. Porcinai, A. Santagostino Barbone, A. Sansonetti, An in situ multi-analytical approach in the restoration of bronze artefacts. Microchem. J. **125**, 151–158 (2016). https://doi.org/10.1016/j.microc.2015.11.018
13. G. Masi, J. Esvan, C. Josse, C. Chiavari, E. Bernardi, C. Martini, M.C. Bignozzi, N. Gartner, T. Kosec, L. Robbiola, Characterization of typical patinas simulating bronze corrosion in outdoor conditions. Mater. Chem. Phys. **200**, 308–321 (2017). https://doi.org/10.1016/j.matchemphys.2017.07.091
14. C. Petiti, L. Toniolo, L. Berti, S. Goidanich, Artistic and laboratory patinas on copper and bronze surfaces. Appl. Sci. **13**(21), 11873 (2023). https://doi.org/10.3390/app132111873
15. T. Kosec, M.B. Leban, P. Ropret, M. FinÅ¡gar, The impact of urban rain on the changes of bare and artificially patinated bronze during 9-year exposure. Environ. Sci. Pollut. Res. **31**(22), 31925–31941 (2024). https://doi.org/10.1007/s11356-024-33369-9
16. P. Letardi, Testing new coatings for outdoor bronze monuments: a methodological overview. Coatings **11**(2), 131 (2021). https://doi.org/10.3390/coatings11020131
17. M.T. Molina, E. Cano, B. RamÃrez-Barat, Protective coatings for metallic heritage conservation: a review. J. Cult. Herit. **62**, 99–113 (2023). https://doi.org/10.1016/j.culher.2023.05.019
18. E. Bernardi, C. Chiavari, C. Martini, L. Morselli, The atmospheric corrosion of quaternary bronzes: an evaluation of the dissolution rate of the alloying elements. Appl. Phys. A **92**(1), 83–89 (2008). https://doi.org/10.1007/s00339-008-4451-0
19. C. Chiavari, K. Rahmouni, H. Takenouti, S. Joiret, P. Vermaut, L. Robbiola, Composition and electrochemical properties of natural patinas of outdoor bronze monuments. Electrochim. Acta **52**(27), 7760–7769 (2007). https://doi.org/10.1016/j.electacta.2006.12.053
20. D. Porcu, S. Innocenti, M. Galeotti, J. Striova, L. Dei, E. Carretti, R. Fontana, Spectroscopic and morphologic investigation of bronze disease: performance evaluation of portable devices. Heritage **5**(4), 3548–3561 (2022). https://doi.org/10.3390/heritage5040184
21. C. Casavola, P. Pappalardi, G. Pappalettera, G. Renna, A fringe projection based approach for corrosion monitoring in metals. Exp. Tech. **42**(3), 291–297 (2018). https://doi.org/10.1007/s40799-018-0234-5
22. C.-M. Popescu, C. Hill, C. Kennedy, Variation in the sorption properties of historic parchment evaluated by dynamic water vapour sorption. J. Cult. Herit. **17**, 87–94 (2016)
23. L.G. Gonzalez, T.J. Wess, The effects of hydration on the collagen and gelatine phases within parchment artefacts. Herit. Sci. **1**(1), 14 (2013)
24. A. Carver-Kubik, J. Reilly, The mechanical behavior of library and archive materials. Mech. Art Mater. Fut. Herit. Sci., **75** (2019)
25. A. Facchini, C. Malara, G. Bazzani, P.L. Cavallotti, Ancient parchment examination by surface investigation methods. J. Colloid Interface Sci. **231**(2), 213–220 (2000). https://doi.org/10.1006/jcis.2000.7138
26. A. Možir, I.K. Cigić, M. Marinśek, M. Strlič, Material properties of historic parchment: a reference collection survey. Stud. Conserv. **59**(3), 136–149 (2014). https://doi.org/10.1179/2047058413y.0000000100
27. M.B. (Haulică), O. Florescu, V. Vasilache, I. Sandu, The comparative study of the state of conservation of two medieval documents on parchment from different historical periods. Materials **13**(21), 4766 (2020). https://doi.org/10.3390/ma13214766
28. L. Krzemień, A. Czyżewska, M. Soboń, R. Kozłowski, L. Bratasz, Risk of climate-induced damage in historic parchment. Herit. Sci. (2020) https://doi.org/10.1186/s40494-020-0360-0

29. A. Papanikolaou, D. Dzik-Kruszelnicka, M. Kujawinska, Spatio-temporal monitoring of humidity induced 3d displacements and strains in mounted and unmounted parchments. Herit. Sci. **10**(1) (2022) https://doi.org/10.1186/s40494-022-00648-y
30. B.N.J. Persson, On the use of surface roughness parameters. Tribol. Lett. **71**(2), 29 (2023). https://doi.org/10.1007/s11249-023-01700-z
31. B. Persson, O. Albohr, U. Tartaglino, A.I. Volokitin, E. Tosatti, On the nature of surface roughness with application to contact mechanics, sealing, rubber friction and adhesion. J. Phys.: Condens. Matter **17**(1), 1–62 (2004). https://doi.org/10.1088/0953-8984/17/1/r01
32. T. Jacobs, T. Junge, L. Pastewka, Quantitative characterization of surface topography using spectral analysis. Surf. Topogr. Metrol. Prop. **5**(1), 013001 (2017). https://doi.org/10.1088/2051-672x/aa51f8
33. P. Podulka, Fast Fourier Transform detection and reduction of high-frequency errors from the results of surface topography profile measurements of honed textures. Eksploat. I Niezawodn. - Maint. Reliab. **23**(1), 84–93 (2021). https://doi.org/10.17531/ein.2021.1.9
34. M. Galeotti, G. Karagiannis, S. Porcinai, A. Santagostino, D3.3. procedures and application of artificial ageing. Technical report, Scan4Reco project, Grant Agreement No: 665091 (2016)
35. S. Mazzocato, D. Cimino, C. Daffara, Integrated microprofilometry and multispectral imaging for full-field analysis of ancient manuscripts. J. Cult. Herit. **66**, 110–116 (2024). https://doi.org/10.1016/j.culher.2023.11.014
36. E.M. Fischer, R. Knutti, Observed heavy precipitation increase confirms theory and early models. Nat. Clim. Chang. **6**(11), 986–991 (2016). https://doi.org/10.1038/nclimate3110
37. P. Faggian, Future precipitation scenarios over Italy. Water **13**(10), 1335 (2021). https://doi.org/10.3390/w13101335
38. Copernicus Climate Change Service: ERA5-Land Monthly Averaged Data from 1950 to Present. https://doi.org/10.24381/CDS.68D2BB30 . https://cds.climate.copernicus.eu/doi/10.24381/cds.68d2bb30 Accessed Accessed: 05-08-2024
39. ARPA Veneto. http://www.arpa.veneto.it/. [Accessed 09-08-2024]